A Model To Predict the Adsorber Thermal Behavior during Treatment of Volatile Organic Compounds onto Wet Activated Carbon

ARTICLE *in* ENVIRONMENTAL SCIENCE AND TECHNOLOGY · DECEMBER 2002

Impact Factor: 5.33 · DOI: 10.1021/es020067h · Source: PubMed

3 AUTHORS, INCLUDING:

Pascaline Pré
CNRS unit GEPEA, Mines Nantes, France
46 PUBLICATIONS **349** CITATIONS
SEE PROFILE

Pierre Le Cloirec
Ecole Nationale Supérieure de Chimie de Re…
313 PUBLICATIONS **6,403** CITATIONS
SEE PROFILE

Environ. Sci. Technol. **2002**, *36,* 4681−4688

A Model To Predict the Adsorber Thermal Behavior during Treatment of Volatile Organic Compounds onto Wet Activated Carbon

P. PRÉ,* F. DELAGE, AND P. LE CLOIREC

Ecole des Mines de Nantes, GEPEA, 4 rue Alfred Kastler, BP 20722, 44307 Nantes Cedex 03, France

A model for adsorption of volatile organic compounds (VOCs) onto a wet activated carbon bed was proposed in this study. This model accounts for temperature changes induced by the reversed and coupled mass-transfer processes of both organic species adsorption and water desorption. Indeed, it was experimentally pointed out that temperature rises, which result from the exothermal nature of the energetic interactions between the organic molecule and the activated carbon surface, are notably reduced when the adsorbent contains an initial moisture of ∼10% in weight. Moreover, it was shown that water rate desorption was enhanced in the presence of organic vapor. This phenomenon may be explained by the displacement of sorbed water by the organic molecules, owing to more intensive interactions with the activated carbon surface. The model proposed was elaborated from a previous comprehensive analysis of the diffusion mechanisms governing VOC adsorption at high concentrations onto a dry activated carbon bed. In a similar way, a theoretical approach was developed to model water desorption during drying of a wet activated carbon bed under pure flowing air. At last, a theoretical depiction of both competitive and reverse processes was outlined. The final model fits reasonably with experimental data relative to both breakthrough curves and thermal wave shape along the bed, even if local temperature change calculation may require some further improvement.

Introduction

Adsorption of volatile organic compounds onto activated carbon is known as an effective technology for air depollution and solvent recovery. Most of the industrial units work under batch conditions, operating with a cyclic adsorption/regeneration system. Most often, regeneration of the adsorbent during the desorption cycle is achieved either by reducing the total pressure in the bed (pressure swing process) or by heating with a stream of hot gas (thermal swing process). However, on solvent recovery units using an activated carbon adsorbent, steam stripping is the most widely used (*1*). This mode of regeneration, which may be considered as a combination of thermal swing and displacement desorption, is well suited because it permits us to increase the desorbate concentration in the effluent and ease the additional separation steps, involving flashing and condensation.

* Corresponding author. Phone: (33)2 51 85 82 68. Fax: (33)2 51 85 82 99. E-mail: Pascaline.Pre@emn.fr.

As a consequence of the steam stripping during the regeneration step, the activated carbon bed contains some residual water at the start of the adsorption cycle. It is of major interest to determine the influence of activated carbon moisture on the separation efficiency of the process during the treatment of air loaded with volatile organic compounds (VOCs).

Furthermore, accounting for the high VOC concentration levels, which are likely to arise in the air feed on solvent recovery units, warming of the bed resulting from the exothermal nature of adsorption has also to be considered. Local temperature rises within the bed may indeed cause both performance degradation and fire hazards. During the last 30 years, incidents involving activated carbon bed ignition in industrial solvent recovery plants were reported (*2-4*). Recent work (*5-7*) pointed out that bed ignition is likely to occur whenever the temperature becomes locally higher than the minimum required to start the oxidation reactions of either the adsorbate or the adsorbent itself. Due to heat accumulating, reaction rates are then accelerated and chain mechanisms set up.

Note that temperature oxidation of some organic adsorbates, particularly those of the ketone group, is far below the self-ignition temperature reported in the literature for the solvent (*6*). Consequently, it clearly appears that, to ensure the efficiency and the safety of the process, control of the temperature maximums reached within the bed under operating conditions is necessary.

For this reason, a main part of our previous work paid attention to characterization of the thermal behavior of the activated carbon bed during adsorption of high VOC concentrations (*8, 9*). A model was developed in order to simulate an activated carbon bed adsorber treating high loads of VOCs (*8*). This model was validated with 38 experimental tests conducted with 7 chemicals from various classes of organic compounds, within a concentration range up to 100 $g \cdot m^{-3}$ and a wide velocity range. The comparison between experimental and theoretical data showed very good agreement, and it proved that such a tool is helpful to prevent ignition risk. However, its application is presently restricted to adsorption of one pure compound, onto a dry activated carbon bed. No interaction in the presence of other volatile components was taken into account in the model. This model has to be improved in order to extend its application to conditions close to those actually met on industrial units.

The main aim of the present study was so to propose a model that accounts for the influence of residual water content of the activated carbon bed to predict its performance and its thermal behavior. The theoretical approach is based on a previous experimental study (*9*) that clarified the modifications induced in the dynamic temperature profiles measured within the bed operating under humid conditions. To get a clear insight into the phenomena involved, water desorption was first analyzed under pure air flowing. VOCs adsorption onto wet activated carbon was afterwards studied.

Theoretical Approach

Mathematical models representative of the column dynamics in nonisothermal conditions require numerical solution of a set of coupled differential equations based on heat and mass balances. Ruthven (*1*) and Tien (*10*) provided a review of the existing mathematical models, available for single-component and multicomponent fixed-bed adsorption systems. Among the most common approaches, the simplest one consists of neglecting both heat- and mass-transfer resistances by assuming that equilibrium is instantaneously

10.1021/es020067h CCC: $22.00
Published on Web 10/04/2002

established (*10*−*12*). However, while the assumption of negligible heat-transfer resistance between the gas and the solid phase is justified, an accurate prediction of adsorption performance requires considering the mass-transfer kinetics.

Because of its simple mathematical form, the linear driving force (LDF) model is commonly used to describe mass-transfer kinetics. According to this model, the mass flux is related to the difference between the equilibrium surface concentration and the average adsorbed-phase concentration. Although the global mass-transfer coefficient is often considered as an adjustable parameter (*13*−*15*), some authors attempted to correlate its value with the diffusion coefficients. For adsorption of large amounts of single species, the contribution of surface diffusion is predominant and expressions of the global coefficient were thus derived (*8*, *16*−*18*). However, in the case of multicomponent adsorption calculations, complications arise because interactions between the species may occur both in mass transfer and in equilibrium data. Consequently, multicomponent mass transfer remains a relatively unexplored field, and the effect of species interactions in dynamic adsorption systems is usually ignored (*10*).

So, even if some experimental studies pointed out the influence of activated carbon moisture on the bed adsorption capacity and its thermal behavior (*9*, *19*−*20*), previous work dealing with how this influence has to be taken into account in a dynamic model is scarce and limited to isothermal conditions (*21*).

Equilibrium Relationships. In a first step, equilibrium relationships for water and organic vapor were established from experimental adsorption data, using the methods described in the Experimental Section.

In the range of relative humidity in air of less than 45%, experimental data showed a linear form of the adsorption equilibrium isotherms. So the water equilibrium relationship used was simply expressed by

$$q_{1e} = \varphi \times 8.52 \times 10^{-4} \exp((21.8 \times 10^3)/RT)C_{1e} \quad (1)$$

Constants involved in the previous equation were found from experimental adsorption data. Owing to the strong interactions with the surface functional groups of the carbon material, an hysteresis appeared during water desorption (*22*−*24*). Thus, to account for the partial amount of water remaining captured in the micropores, a corrective parameter φ was introduced.

It was experimentally found that, for initial weight moisture content less than 10%, VOC's adsorption capacity on the wet activated carbon is unchanged compared to the dry one (*9*). Because no interactions effect due to the presence of water was revealed on the VOCs equilibrium data, the classical temperature-dependent form of the Langmuir equation was applied:

$$q_{2e} = \frac{q_m b_0 \exp(A/RT)C_{2e}}{1 + b_0 \exp(A/RT)C_{2e}} \quad (2)$$

The appropriate set of constants q_m, b_0, and A were determined from equilibrium isotherms measured on the dry activated carbon.

Intrapellet Mass-Transfer Rates. The kinetics sorption of water and organic molecules on activated carbon was based on the linear driving force mass-transfer model. The rate constants were expressed by considering the differences in the mechanisms involved during sorption of either water or organic vapor.

According to recent work (*25*−*27*), water adsorption proceeds primarily at the functional groups located at the entrance of the micropores, which are interstices between the plane graphite layers. Thus, irreversible chemisorption of water molecules initially occurs with the functional groups. Further, these hydrophilic sites act as nucleation sites leading to formation of water molecule clusters via hydrogen bonding. When adsorption is occurring, water clusters grow in the amorphous region and, beyond a critical size, attain a sufficient dispersive energy with the carbon atoms to enter the micropores (*24*). According to Do and Do (*26*), capillary condensation is likely to occur only at high relative humidity, of ∼90%.

Several authors (*22*−*24*) have mentioned that the LDF model is convenient to describe the adsorption/desorption rate of air humidity onto activated carbon. So, in a similar way, it was primarily proposed to formalize the intrapellet water desorption kinetics using the following equation:

$$\rho_{bed}(\partial q_1/\partial t) = k_1(C_1 - C_{1e}) \quad (3)$$

According to Lin and Nazaroff (*21*), the surface diffusivity contribution does not exceed 30% of the total diffusivity in the case of water vapor adsorption at less than 90% relative humidity and this contribution is reduced when water sorbate concentrations are low. So, given the low initial weight moisture of the adsorbent tested in our experimental conditions, less than 10%, the mass transfer was supposed to be limited by water molecule diffusion in the micropores.

Desorption of water clusters from the secondary sites located within the micropores was supposed to be governed by Knudsen diffusion. The mass-transfer coefficient was then expressed according to Treybal (*29*):

$$k_1 = 60D_1/{d_p}^2 \quad (4)$$

where D_1 is the porous diffusion coefficient given by

$$D_1 = (\epsilon_p/\tau_p)9.7 \times 10^{-8} r_{pore}[T/M]^{0,5} \quad (5)$$

As the tortuosity value is uncertain, ϵ_p/τ_p was initially considered as an adjustable parameter in the model.

In the presence of organic vapors, experimental findings showed that water desorption rate was notably enhanced. This phenomenon is described in detail in ref *9*. The activated carbon has indeed a greater affinity with organic species than water because adsorption of organic molecules proceeds directly via dispersive forces induced by strong electrostatic interactions with atoms of the carbon surface (*1*).

So that, to account for the preferential occupation of the adsorption sites with an organic molecule, the classical form of the LDF model applied to water desorption rate was modified. A pondering parameter related to the partial filling of the volume of the micropores with the organic vapor was introduced in the linear driving force expression in order to account for water desorption acceleration. The desorption rate of water occurring during VOC adsorption was thus expressed as follows:

$$\rho_{bed}(\partial q_1/\partial t) = k_1[C_1(1 - W/W_0) - C_{1e}] \quad (6)$$

In contrast, experimental results showed that whether the bed material was prehumidified or not, the VOC adsorption rate remains almost identical. So, modeling of the VOC adsorption rate in the presence of water is based on the unmodified form of the LDF, which was successfully applied in the case of adsorption of the single compound:

$$\partial q_2/\partial t = k_2(q_{2e} - q_2) \quad (7)$$

In the last equation, the mass-transfer coefficient k_2 may be considered as a lumped quantity, combining external mass transfer and surface diffusion. Its expression was derived from the same correlation as that assessed in our previous

work dealing with adsorption of VOCs onto a dry activated carbon bed (*8*):

$$k_2 = 60D_2/{d_p}^2 \quad (8)$$

where

$$D_2 = 1.23 \times 10^{-9} U_0 \exp[(-1.694 \times 10^{-4} + 0.45/RT)\Delta H_2] \quad (9)$$

Mass and Heat Balances over the Bed. Macroscopic balances representative of the conservation of mass and energy were derived, based on the following assumptions, usually admitted in models proposed for fixed-bed systems in the literature (*1, 10*): (1) The pressure drop through the bed is negligible. (2) The flow pattern is described by the plug flow model. (3) The physical properties of the adsorbent are considered constant. (4) Heat accumulation in the gas phase is negligible.

Conservation of species was expressed over an elementary element volume of the bed, considering transient conditions:

$$\begin{bmatrix}\text{change in moles of species } i\\ \text{in the gas phase per unit of}\\ \text{time in the elementary bed volume}\end{bmatrix} + \begin{bmatrix}\text{change in moles of species } i\\ \text{in the solid phase per unit of}\\ \text{time in the elementary bed volume}\end{bmatrix} + \begin{bmatrix}\text{change in the molar}\\ \text{gas flow rate across the}\\ \text{elementary volume}\end{bmatrix} = 0$$

$$\Rightarrow \epsilon_{bed}\frac{\partial C_i}{\partial t} + \rho_{bed}\frac{\partial q_i}{\partial t} + U_0\frac{\partial C_i}{\partial z} = 0 \qquad i = 1, 2 \quad (10)$$

The energy balance accounts for the enthalpy variation of the flowing gas, heat accumulation within the wet pellets and heat losses at the wall:

$$\begin{bmatrix}\text{heat acumulated in the solid phase}\\ \text{in the bed elementary volume per unit of time}\end{bmatrix} + \begin{bmatrix}\text{change in the enthalpy}\\ \text{of the gas flowing across}\\ \text{the elementary volume}\end{bmatrix} = -\begin{bmatrix}\text{heat absorbed per unit of time}\\ \text{due to water desorption}\end{bmatrix} + \begin{bmatrix}\text{heat released per unit of time}\\ \text{due to VOC adsorption}\end{bmatrix} - \begin{bmatrix}\text{heat losses at the wall}\\ \text{per unit of time}\end{bmatrix}$$

$$\Rightarrow \rho_{bed}(C_{ps} + q_1C_{p1} + q_2C_{p2})\frac{\partial T}{\partial t} + U_0\rho_g C_{pg}\frac{\partial T}{\partial z} = \rho_{bed}\left(\Delta H_1\frac{\partial q_1}{\partial t} - \Delta H_2\frac{\partial q_2}{\partial t}\right) - \frac{4h_0}{D}(T - T_0) \quad (11)$$

Equations 6, 7, 10, and 11 form a set of five partial differential equations to be numerically solved to simulate changes in species concentrations and temperature with time along the bed.

After simple drying under flowing air, it was experimentally proved that some water remains captured in the activated carbon bed. This residual part of humidity is likely to be bound with the functional groups of the carbon surface, or condensed with the adsorbent micropores, or both. Only thermal treatment enables total water desorption from the adsorbent.

So that, considering that only 75% of the total water content of the material could be desorbed, the initial conditions used are

$$C_1(z,0) = C_{01} \qquad C_2(z,0) = C_{02} \qquad T(z,0) = T_0$$
$$q_1(z,0) = 0{,}75q_{01} \qquad q_2(z,0) = 0$$

The boundary conditions for $t > 0$ are

$$C_1(0,t) = 0 \qquad C_2(0,t) = C_{02} \qquad T(0,t) = T_0$$
$$\partial C_1(L,t)/\partial z = 0 \qquad \partial C_2(L,t)/\partial z = 0$$

The set of PDEs was written in dimensionless form. The spatial discretization was performed using the Keller box scheme, and the method of lines was employed to reduce the PDEs to a system of ordinary differential equations. The resulting system is solved using a backward differentiation formula method.

Rational validation of the coupling model requires an intermediary step to verify the correct prediction of single water desorption rate and temperature drops induced by the endothermic process. For that purpose, concentrations of the VOC in gas and pellet phases, as well as the partial pore filling parameter, were first considered null. Accounting for mass balances relative to water only and heat conservation, the set of equations to be solved was then reduced to three PDEs. The accuracy of the single water desorption calculation was thereafter evaluated from experimental data obtained under pure flowing air. At last, the complete model, describing the coupling mechanisms of both VOC and water intrapellet transfers, was tested.

Experimental Section

Activated Carbon Material. The adsorbent used was Picactif NC60, a granular carbon manufactured by Pica Co (Levallois-Perret, France). Its physical properties are specified in Table 1. Taken just as is, the carbon is wet, with a water content of ~9.8 wt %. Owing to a drying treatment at 105 °C for 24 h, the residual water content ranges below 1%. The dried activated carbon was then regarded as the reference material to be compared with wet samples.

Equilibrium Isotherm Data. The equilibrium water adsorption isotherms were obtained using differential scanning calorimetry coupled to thermogravimetry analysis (model Setaram TG-DSC 111). A sample of the adsorbent material was placed in a cell whose temperature was controlled. The sample was preliminarily heated to 120 °C to remove its initial water content. After cooling, a constant air flow with a known amount of moisture passed through the cell. The sample mass variation data were continuously registered until equilibrium was attained. The adsorption capacities were thus determined for gas moisture varying from 0 to 100% and at temperatures of 20, 40, and 60 °C.

Figure 1 shows that, in the range of water content in the activated carbon of less than 10%, a good agreement is obtained between the water adsorption isotherm data and

TABLE 1. Physical Properties of the Adsorbent

property	Picactif NC 60
raw material	coconut shell
grain size range (mm)	0.55−1.0
moisture as packed (%)	9.8
BET surface area ($m^2 \cdot g^{-1}$)	1117
pore volume ($cm^3 \cdot g^{-1}$)	0.538
mean microporous diameter (nm)	0.68
calorific capacity ($J \cdot kg^{-1} \cdot K^{-1}$)	880
oxidation temperature (°C)	203

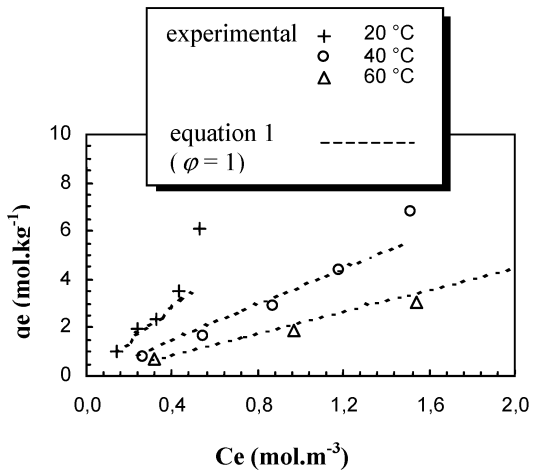

FIGURE 1. Isotherms of water adsorption.

TABLE 2. Constants Involved in the Langmuir Equilibrium Relationship

VOC	q_m (mol·kg^{-1})	$b_0 \times 10^7$ (m^3·mol^{-1})	$A \times 10^{-3}$ (J·mol^{-1})
acetone	5.921	228	31.4
toluene	4.609	4.06	45.5
1,2-dichloroethane	5.322	1.63	47.5

TABLE 3. Enthalpies Data for Water Desorption (ΔH_1) and VOC's Adsorption (ΔH_2)

compound	enthalpy (kJ·mol^{-1})
water	39.7
acetone	−50.6
toluene	−63.1
1,2-dichloroethane	−51.2

the temperature-dependent linear equilibrium relationship, given by eq 1.

Equilibrium data for VOC adsorption onto the dried activated carbon were determined in batch reactors operating at constant temperature, from 20 to 80 °C. The temperature-dependent form of the Langmuir equation (eq 2) was proved to fit well the experimental equilibrium data of the organic compounds tested. The set of constants involved is given in Table 2.

Heats of Adsorption and Desorption. The TG-DSC apparatus was also used for the determination of heat released during adsorption of a VOC. A sample of the adsorbent material was first placed in a cell and heated to 120 °C under inert atmosphere. This preliminary step allowed removal of the residual water content of the material. After cooling, the adsorption energies were determined at a constant temperature of 20 °C. A gaseous mixture composed of VOC at a concentration of 50 g·m^{-3} diluted in helium continuously flowed through the sample until saturation of the adsorbent. The mass variations and heat released were simultaneously collected.

Water desorption enthalpies were obtained by heating a wet activated carbon sample from 20 to 400 °C. As the total heat amount absorbed results from both the endothermic effect of water desorption and the variation in the material calorific capacity, a blank test was performed using a dried sample in order to subtract this last contribution.

All these measurements were reproducible with a relative error of ∼5%. Enthalpy data are specified in Table 3.

Experimental Setup. Both adsorption and water desorption tests were conducted on the experimental setup shown

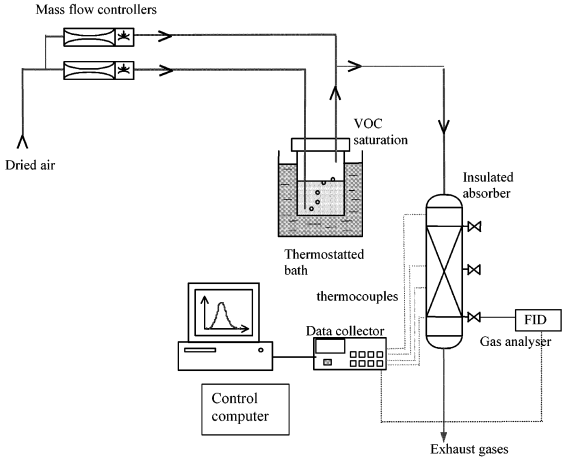

FIGURE 2. Diagram of the experimental setup.

TABLE 4. Operating Conditions

test	gas superficial velocity U_0 (m·h^{-1})	initial water$_{(1)}$ content q_{01} (mol·kg^{-1})	nature of the organic species$_{(2)}$	VOC concn at the inlet (g·m^{-3})
A1	500	3.55	none	0
A2	2000	5.44	none	0
A3	500	5.44	none	0
B1	500	5.44	acetone	25
B2	500	5.44	acetone	50
B3	500	3.55	acetone	50
B4	500	4.56	acetone	48
B5	500	5.44	acetone	75
B6	500	5.44	toluene	50
B7	500	5.44	1,2-dichloroethane	50

in Figure 2. A glass column of 46-mm inner diameter is packed with either the wet or dry adsorbent up to 200 mm in height. The column is insulated to limit heat losses at the wall. So, using the experimental method described by Schork and Fair (*11*), the global heat-transfer coefficient at the wall was evaluated at 4 W·m^{-2}·K^{-1}. VOC vapor was produced by bubbling air through a vessel filled with the organic liquid solvent. The VOC vapor was diluted in a dried air flux and mass flow controllers provided an accurate adjustment of the pollutant concentration desired. The VOC concentration in the gas phase was continuously measured by a flame ionization detector (Cosma 355) at several heights. Breakthrough time was determined when the time of the exit pollutant concentration becomes equal to 10% of that at the inlet.

The temperature was measured by means of K thermocouples placed along the central axis of the column. The operating conditions tested are presented in Table 4.

Modeling Results and Discussion

Modeling Water Desorption under Pure Flowing Air. Dynamic water desorption under pure flowing air was carried out through tests A1−A3. While no thermal effect is observed when dry air flows onto a dry activated carbon bed, a temperature drop is measured when dry air flows onto a humid activated carbon, as shown in Figures 3−5. The temperature decrease is induced by the desorption of water molecules, which is an endothermic phenomenon. Spreading of the temperature curves measured might be explained by simultaneous adsorption of water molecules being desorbed upstream along the bed.

At the end of these experiments, the amount of residual water still present in the activated carbon grains was determined by weighing, before and after, samples having

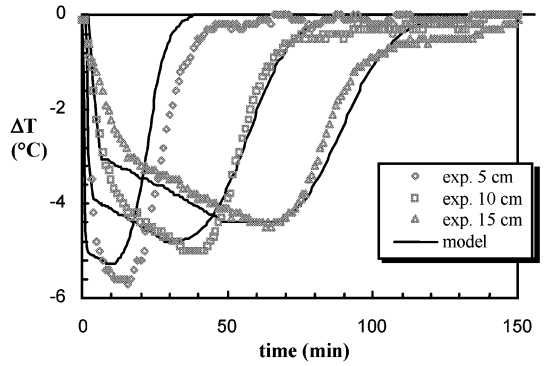

FIGURE 3. Computed and experimental temperature profiles (test A1).

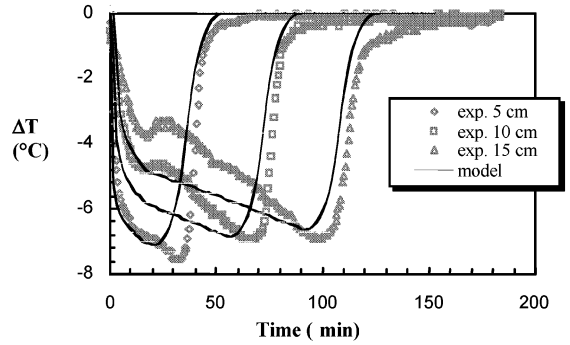

FIGURE 4. Computed and experimental temperature profiles (test A2).

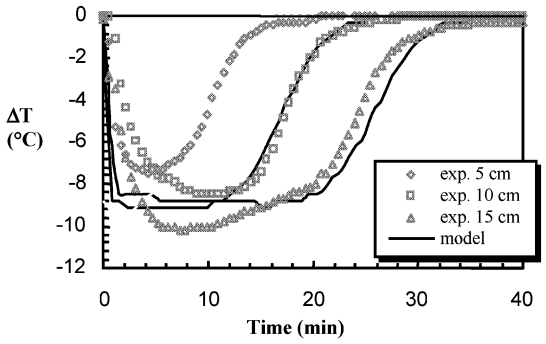

FIGURE 5. Computed and experimental temperature profiles (test A3).

been dried in an oven at 105 °C. Thus, it was shown that at the end of tests A1 and A3, activated carbon grains still contain respectively 1.8% and 2.1% moisture. This means that only 72% of the initial amount of water was desorbed during test A1 and 78% during test A3. This part of residual moisture corresponds to water molecules that were strongly bound to the activated carbon surface, as those primarily chemisorbed with the functional groups. Indeed, assuming that each functional group is bonded with one water molecule, and accounting for the concentrations of phenols and basic functions (0.45 and 0.61 mol·kg^{-1}, respectively) of the activated carbon employed, the residual fraction of water should be ~1 mol·kg^{-1}, i.e., 1.8%. This value is close to the actual water content remaining in the adsorbent after dynamic desorption tests.

Parameters of the model for single water desorption were adjusted in order to fit with one temperature profile observed at 100 mm in height during bed drying under pure flowing air (test A1). The agreement between the modeling results and the whole experimental data obtained during tests A1−A3, was thereafter verified.

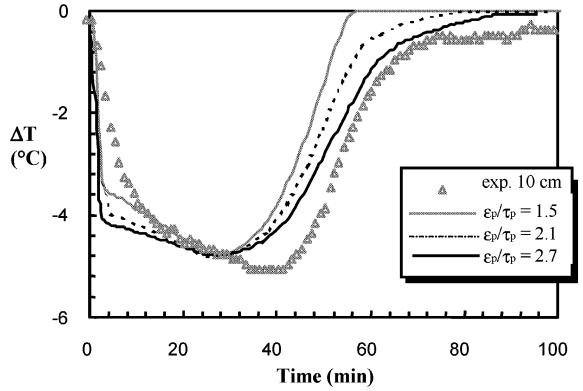

FIGURE 6. Effect of ϵ_p/τ_p parameter on temperature curve ($z = 100$ mm, test A1).

Parameter Sensitivity. Conformation of the model with experimental data was examined after previous adjustment of the unknown parameters ϵ_p/τ_p and φ, involved respectively in the estimation of the porous diffusion coefficient D_1 (eq 5) and in the water equilibrium relationship accounting for an hysteresis loop (eq 1).

Simulation results pointed out the influence of the first parameter on the desorption rate: the higher ϵ_p/τ_p, the higher the porous diffusion coefficient and so the faster the desorption rate. This effect is reflected in the breaktrough curves' broadening as well as in the thermal wave amplitude. Figure 6 compares temperature profiles computed with different values of $\epsilon_p/\tau_{p,}$. For lower values of ϵ_p/τ_p, the area over the temperature curve is reduced although any change of the temperature minimums is observed. This is significant of the lessening of the endothermic heat flux absorbed by an elementary volume of the bed. Furthermore, note that whatever the ϵ_p/τ_p value, a time lag is observed between the calculated temperature curves and the experimental one, suggesting that the desorption kinetic is still overestimated. This may be explained by the initial nonadjustment of the φ parameter, representative of the displacement of the partitioning equilibrium due to hysteresis desorption. φ is equal to 1, the equilibrium water concentration in air C_{1e} involved in the LDF model (eq 3) is likely to be overestimated, and computed water desorption rate is consequently accelerated. Nevertheless, these results permitted prior selection of the best ϵ_p/τ_p value, following the shape of the experimental curve. Finally, 2.1 was the value retained because the experimental temperature profile may be properly reproduced, provided a lag is included in the calculation results. However, assuming that the intraparticle porosity ϵ_p is ~0.6, the tortuosity then becomes inferior to 0.3, which is far below the physical range usually reported, from 2 to 6. It appears then more convenient to consider this parameter only as a correcting factor, casting doubt on its physical meaning.

The φ parameter was thereafter adjusted in regard to the minimal mean square deviation observed between the experimental and computed temperature changes with time. An optimal value of 1.174 was found (Figure 7).

Comparison between Experimental and Theoretical Results. The predictive ability of the model for water desorption under pure flowing air was evaluated from temperature and sorbed water concentration profiles measured at different heights in the bed during tests A1−A3. For test A1, comparison of experimental and theoretical temperature profiles is presented in Figure 3. Figure 8 enables us to compare the experimental and computed dynamic water desorption curves. For activated carbon whose residual water content is far less than 10%, a correct agreement is observed. Figures 4 and 5 exhibit measured and computed temperature profiles

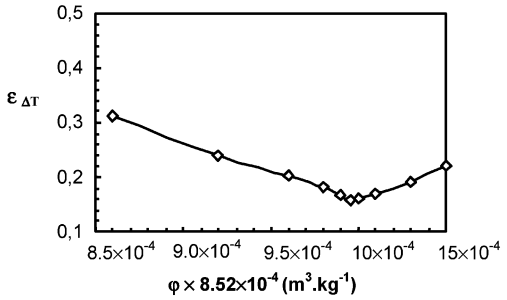

FIGURE 7. Effect of φ parameter on the mean square deviation between experimental and theoretical temperature curves ($z = 100$ mm, test A1).

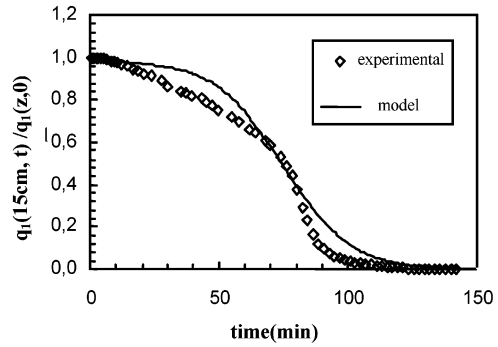

FIGURE 8. Comparison of computed and experimental sorbed water concentration changes ($z = 150$ nm, test A1).

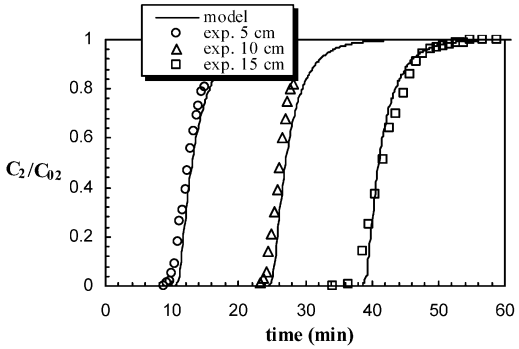

FIGURE 9. Experimental and computed toluene breakthrough curves (test B6).

for intrinsic humidity close to 10% (tests A2 and A3). Under these conditions, deviations are observed but especially on the decreasing part of the temperature curves, while the increasing part fits well with the experimental data. So the observed trends for thermal wave amplitudes and propagation are still well represented with the model. The initial deviations may be related to the difference in the physical state of sorbed water. Indeed, for moisture content close to 10%, a fraction of the sorbed water may be condensed within the micropores. Furthermore, it is worth noting that gas velocity was increased 4 times under the operating conditions of test A3 compared to those of tests A1 and A2. High relative gas humidity was then measured during this test, locally greater than 45%, which corresponds to the upper limit for the linear equilibrium relationship.

VOCs Adsorption onto Wet Activated Carbon. After models were separately developed to describe VOC adsorption onto dried activated carbon and single water desorption under pure flowing air, a theoretical depiction of the both coupled processes was attempted. This model is based on the assumption that water molecules desorbed faster in the presence of organic vapors owing to their weaker interactions with the activated carbon surface. Simulation results presented and discussed in this section would permit verification of the validity of such a supposition.

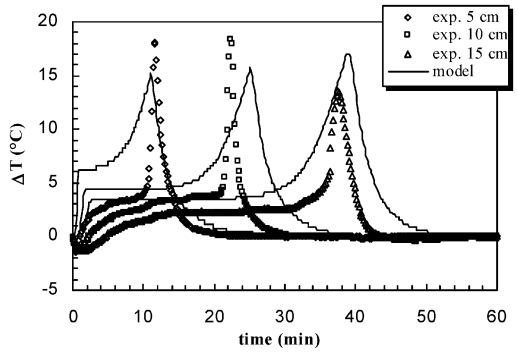

FIGURE 10. Experimental and computed temperature curves (test B6).

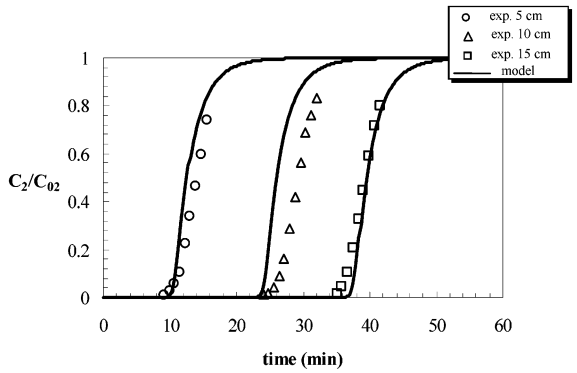

FIGURE 11. Experimental breakthrough curves (same conditions as test B6 but dried adsorbent).

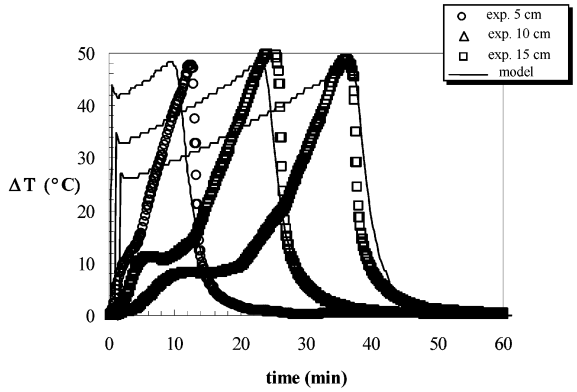

FIGURE 12. Experimental temperature curves (same conditions as test B6 but dried adsorbent).

Figures 9−12 permit comparison of simulation results with experimental data in the case of adsorption of toluene onto wet and dry activated carbon with the same conditions as test B6. The model provides a good prediction of the experimental breakthrough curves observed during adsorption of the VOC onto wet or dry activated carbon (Figures 9 and 11). This is not surprising since the effect of water on the VOC adsorption capacity and breakthrough times was not found significant under the experimental conditions tested (9). On the other hand, Figures 10 and 12 illustrate the ability of the model to reproduce the modifications induced by the endothermic effect of water desorption on temperature profiles. The agreement between the experimental and computed temperature curves is not as good as that expected since deviations of a few degrees may be observed.

However, it is worth noting that temperature profiles are strongly modified during adsorption onto either wet or dried

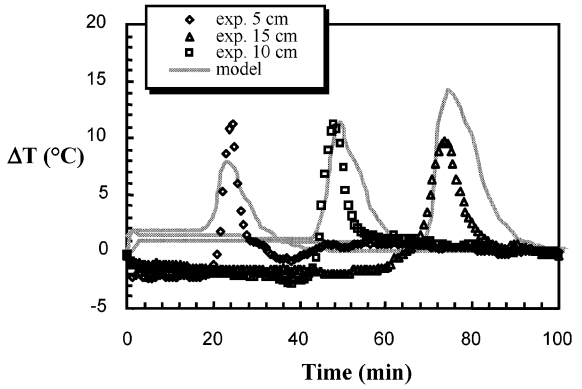

FIGURE 13. Experimental and computed temperature profiles (test B1).

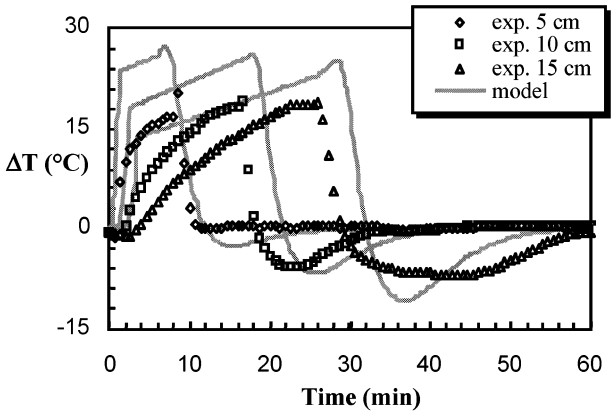

FIGURE 14. Experimental and theoretical temperature profiles (test B5).

activated carbon. In particular, temperature changes are notably lowered while thermal waves are narrowed. Thus, in the case of toluene adsorption onto dry activated carbon, with the same inlet conditions, temperature rises reached 50 °C (Figure 12) whereas they do not exceed 20 °C on the wet material (Figure 10). So, even if prediction in local temperature changes with time is not too accurate, the model conforms well with the qualitative trends observed.

In the case of acetone adsorption at concentrations less than 50 g·m^{-3}, the quality prediction of the model is comparable with that observed with toluene (Figure 13). This result is noticeable since acetone is a hydrophilic compound whereas toluene is hydrophobic. In these conditions, the solubility of the organic compound in water is proved to have no significant impact on the transfer mechanisms. This result is in accordance with the conclusions of Biron and Evans (*30*) showing that water solubility does not have a major influence on dynamic adsorption of organic vapors onto moisturized carbon.

On increase of the inlet acetone concentration to 50 g·m^{-3}, the form of the thermal wave is strongly modified, but the model properly fits with the shape of the experimental curves. In Figure 14, one may notice a negative thermal amplitude representative of the endothermic phenomenon, which occurs after the positive one. The prior positive peak is relevant to the adsorption of the organic compound. As acetone concentration in air measured during the breakthrough remains always below the one at the inlet, acetone desorption is unlikely to arise. So, only water desorption causes the negative temperature changes. In the same figure, the reported temperature deviations show that the endothermic heat flux is underestimated. This leads to the conclusion that water desorption kinetics is likely to be

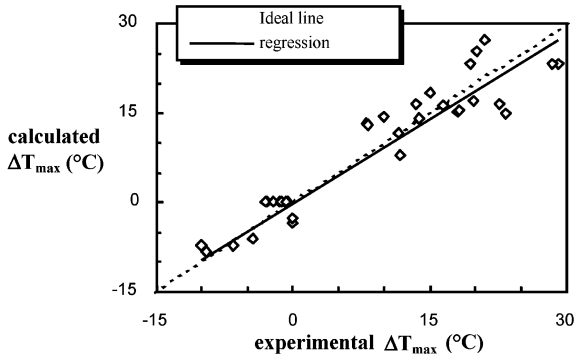

FIGURE 15. Comparison between calculated and experimental maximal temperature rises (tests B1−B7).

underestimated although the LDF model was modified in order to account for water desorption enhancement in the presence of organic vapor.

For all operating conditions tested, Figure 15 permits comparison of experimental and theoretical temperature extrema reported at different heights within the bed (50, 100, and 150 mm). Typically, for all of the experiments conducted on wet activated carbon, the positive thermal amplitudes do not exceed 25 °C and deviations observed are always inferior to 10 °C. For the same inlet conditions, temperature rises measured during adsorption tests onto dry material were 2−3 times higher (*8, 9*).

So, although predicted temperature rises during adsorption onto wet activated carbon remain somewhat imprecise, one may conclude that the model is suitable to describe global changes in thermal behavior observed with operating conditions. So the assumptions advanced to describe the coupling of mass-transfer processes seem to be correct. It is suggested that improvement in calculation results may be obtained by accounting for the dependence of water equilibrium partitioning upon organic sorbate concentration.

Acknowledgments

This work was supported by ADEME (Agence de l'Environnement et de la Maîtrise de l'Energie, France) under Contract 9774100. We thank Pica Co and G. Dagois, the Managing Director, for providing samples and information on activated carbon.

Nomenclature

C_1, C_2	concentration of water and VOC in the gas phase (mol·m^{-3})
Cp_s	specific heat of the activated carbon (J·kg^{-1}·K^{-1})
Cp_1, Cp_2	adsorbates heat capacities (J·mol^{-1}·K^{-1})
Cp_g	specific heat of air (J·kg^{-1}·K^{-1})
d_p	mean particle diameter (m)
D_1, D_2	diffusion coefficients (m^2·s^{-1})
D	column diameter (m)
h_0	overall heat-transfer coefficient (W·m^2·s^{-1})
k_1, k_2	mass-transfer coefficient (s^{-1})
M	molar mass of water (g·mol^{-1})
q_1, q_2	adsorbates concentration (mol·kg^{-1})
r_{pore}	pore radius (nm)
R	gas constant (8.314 J·mol^{-1}·K^{-1})
t	time (s)

T	temperature (K)
U_0	superficial gas velocity at the inlet ($m \cdot s^{-1}$)
W	volume of VOC adsorbed ($m^3 \cdot kg^{-1}$)
W_0	microporous volume of the adsorbent ($m^3 \cdot kg^{-1}$)
ϵ_{bed}	void fraction of the bed
ϵ_p	intragranular porosity
ΔH_1, ΔH_2	desorption enthalpy of water, adsorption enthalpy of VOC ($J \cdot mol^{-1}$)
ρ_g	air density ($kg \cdot m^{-3}$)
ρ_{bed}	bed density ($kg \cdot m^{-3}$)
τ_p	tortuosity
indexes	
0	at the inlet
1	relative to water
2	relative to the organic compound

Literature Cited

(1) Ruthwen, M. D. *Principles of adsorption and adsorption processes*; John Wiley & Sons: New York, 1984.
(2) Naujokas, A. A. *Plant Oper. Prog.* **1985**, *4*(2), 120−126.
(3) Wildman, J. *Proceedings of an International Conference on Carbon*; University of Newcastle Upon Tyne, United Kingdom, 1988.
(4) *Chemical safety alert*; EPA-550-F-97_002e; U.S. Environmental Protection Agency, Chemical Emergency preparedness and prevention office, U.S. Government Printing Office: Washington, DC, 1997.
(5) Akubuiro, E. C., *Ind. Eng. Chem. Res* **1993**, *32*, 2960−2968.
(6) Delage, F. Echauffement des lits de charbon actif lors de l′adsorption de composés organiques volatils: étude expérimentale et modélisation. Ph.D. Thesis, Université de Poitiers, Ecole des Mines de Nantes, France, 2000.
(7) Henning, K. D.; Bongartz, W.; Degel, J. CarboTech Co., Essen, Germany.
(8) Delage, F., Pré, P.; Le Cloirec, P. *Environ. Sci. Technol.* **2000**, *34* (22), 4816−4821.
(9) Delage, F.; Pré, P.; Le Cloirec, P. *J. Environ. Eng.* **1999**, *125* (12), 1160−1167.
(10) Tien, C. *Adsorption calculations and modelling*; Butterworth-Heinemann: Washington, 1994.
(11) Shork, J. M.; Fair, J. R. *Ind. Eng. Chem. Res.* **1988**, *27* (3), 457−469.
(12) Amundson, N. R.; Aris, R.; Swanson, R. *Proc. R. Soc. Ser. A.* **1965**, *286*, 129−139.
(13) Jacob, P.; Tondeur, D. *Chem. Eng. J.* **1983**, *26*, 41−58.
(14) Luo, L.; Bailly, M. *Rev. Gén. Therm.* **1996**, *35*, 693−697.
(15) Pan, C. Y.; Basmadjian, D. *Chem. Eng. Sci.* **1967**, *22*, 285−297.
(16) Ruthwen, D. M.; Garg, D. R.; Crawford, R. M. *Chem. Eng. Sci.* **1975**, *30*, 803−810.
(17) Yoshida, H.; Ruthwen, D. *Chem. Eng. Sci.* **1983**, *38* (6), 877−884.
(18) Huang, C. C.; Fair, J. R. *AIChE J.* **1988**, *34* (11), 1861−1877.
(19) Huang, C. C.; Hwu, T. L.; Hsia, Y. S. *J. Chem. Eng. Jpn.* **1993**, *26* (1), 21−27.
(20) Hall, C. R.; Holmes, R. J.; Lawston, I. W. *Adsorp. Sci. Technol.* **1991**, *8* (2), 69−74.
(21) Lavanchy, A.; Stoeckli, F. *Carbon* **1999**, *37*, 315−321.
(22) Lin, T. F.; Nazaroff, W. W. *J. Environ. Eng.* **1996**, *122*, 176−182.
(23) Harding, A. W.; Foley, N. J.; Norman, P. R.; Francis, D. C.; Thomas, K. M. *Langmuir* **1998**, *4*, 3858−3864.
(24) Cossarutto, L.; Zimny, T.; Kaczmarczyk, J.; Siemieniewska, T.; Bimer, J.; Weber, J. V. *Carbon* **2001**, 2339−2346.
(25) Iiyama, T.; Ruike, M.; Kaneko, K. *Chem. Phys. Lett.* **2000**, *331* (5/6), 359−364.
(26) Do, D. D; Do, H. D. *Carbon* **2000**, *38*, 767−773.
(27) Müller, E. A.; Gubbins, K. E. *Carbon* **1998**, *36* (10), 1433−1438.
(28) Stoeckli, F.; Currit, L.; Laederach, A.; Centeno, T. A. *J. Chem. Soc., Faraday Trans.* **1994**, *90* (24), 3689−3691.
(29) Treybal, R. E. *Mass-transfer operations*; McGraw-Hill Int.: New York, 1980.
(30) Biron, E.; Evans, M. J. B. *Carbon* **1998**, *36* (7−8), 1191−1197.

Received for review March 22, 2002. Revised manuscript received August 11, 2002. Accepted August 20, 2002.

ES020067H